August 27-31, 2023
FLORENCE - ITALY
ICWE 16
16th International Conference on Wind Engineering

Kármán vortex effect on galloping instability of cylinders

Thinzar Hnin [1], Tomomi Yagi [2], Hisato Matsumiya [3], Kyohei Noguchi [4], Rintaro Kyotani [5]

[1]*Graduate Student, Kyoto University, Kyoto, Japan, thinzar.hnin.58n@st.kyoto-u.ac.jp*
[2]*Professor, Kyoto University, Kyoto, Japan, yagi.tomomi.7a@kyoto-u.ac.jp*
[3]*Associate Professor, Kyoto University, Kyoto, Japan, matsumiya.hisato.4y@kyoto-u.ac.jp*
[4]*Assistant Professor, Kyoto University, Kyoto, Japan, noguchi.kyohei.7z@kyoto-u.ac.jp*
[5]*Graduate Student, Kyoto University, Kyoto, Japan, kyotani.rintaro.28a@st.kyoto-u.ac.jp*

ABSTRACT:
To investigate the effect of Kármán vortex on the galloping instability of a rectangular cylinder, the Kármán vortex shedding intensity was changed by cutting the corners. Wind tunnel tests were conducted to obtain the response amplitude and aerodynamic force characteristics under stationary and vibrating conditions. The onset reduced wind velocity of galloping was found to increase while Kármán vortex shedding intensity was reduced by cutting the corners and the inverse of Strouhal number was also decreased, which conflicted with a well-known fact that the galloping onset was controlled by the inverse of Strouhal number. This is probably because the motion-induced vortices influenced the vibration of the section when Kármán vortex shedding was reduced.

Keywords: motion-induced vortex, Kármán vortex, galloping, rectangular cylinders, corner-cut

1. INTRODUCTION

The separation and reattachment of the shear layers depend on the side ratio (*B/D*, where *B* is the width and *D* is the depth of the section) of a rectangular cylinder and the Reynolds number. This flow separation and reattachment create vortices behind the cylinder. One type of these vortices, which is known as Kármán vortex, causes Kármán vortex-induced vibration (KVIV). On the other hand, the KVIV was suppressed when the corners of a rectangular cylinder were cut into a single recession shape (Shiraishi et al., 1988). Therefore, cutting the corners has some effect on the Kármán vortex shedding. According to previous research, the onset of galloping instability also starts from the reduced wind velocity characterized by the Kármán vortex shedding frequency (1/*St*, *St* = Strouhal number) when the Scruton number is small (Scruton, 1968). Hence, Kármán vortex plays an important role in the vibration of a rectangular cylinder. In this study, three cylinders were prepared (Rectangular, Single Recession, and Triple Recession) as shown in Fig. 1 to provide different Kármán vortex shedding intensities. The effect of Kármán vortex on the galloping instability was studied based on the response amplitude and aerodynamic damping. Finally, the aerodynamic interaction between the vortices and galloping instability were investigated.

2. SETUP OF WIND TUNNEL TESTS

In this study, a room-circuit Eiffel-type wind tunnel of 1.0 m (width) and 1.8 m (height) was used. Static force measurement, vertical 1DOF free vibration, and forced vibration tests were carried out for an attack angle of 0° under the smooth flow condition. The upstream turbulence intensity was below 0.5%. The side ratio of Rectangular was 1.5 (B = 135 mm, D = 90 mm). For the forced vibration test, the vibration frequency was 2.6 Hz and the vibration double amplitude was 0.1D. The structural parameters used in the free vibration test; equivalent mass (m) was 6.8 kg/m, natural frequency (f) was 4.6 Hz, logarithmic decrement in structural damping ($\delta_{\eta\,(2A_\eta\,=\,2\mathrm{mm})}$) was 0.0043, and 0.029, respectively. The displacement amplitude in the vertical direction is defined as A_η (mm). The Scruton number (Sc), is calculated as follows:

$$Sc = \frac{2m\delta_\eta}{\rho D^2} \tag{1}$$

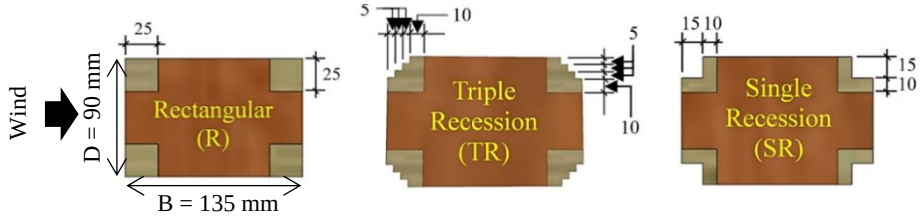

Figure 1. Illustration of the test models.

3. KÁRMÁN VORTEX SHEDDING INTENSITY AND STROUHAL NUMBER

Static force measurement was carried out for a wind velocity of 10.8 m/s (Re = 64.8×10^3). In the studied sections, Reynold number dependency was not observed between 36×10^3 and 64.8×10^3. The Kármán vortex shedding intensity (C'_{Fy}) which is the fluctuating transverse force due to the Kármán vortices and the Strouhal number (St) were calculated according to Eqs. (2) and (3). The C'_{Fy} of Rectangular decreased by about 55 % and 86 % when the corners of a rectangular cylinder were cut into Triple Recession and Single Recession. Besides, the Strouhal number steadily increased (Fig. 2). Since 1/St provides the onset of the KVIV, Single Recession is likely to have the lowest onset reduced wind velocity among the three sections.

$$C'_{Fy} = \frac{F_y(t)_{std}}{0.5\rho U^2 BL} \tag{2}$$

$$St = \frac{f_s D}{U} \tag{3}$$

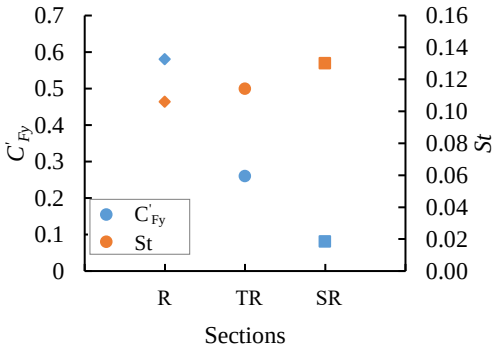

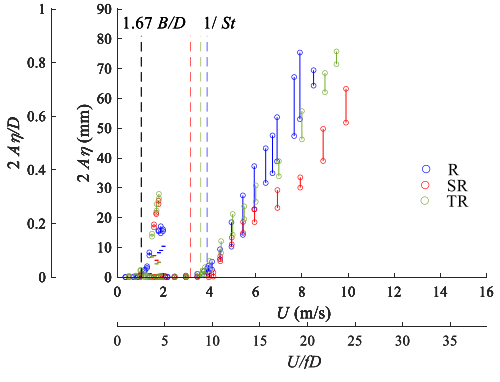

Figure 2. Kármán vortex shedding intensity and Strouhal number. **Figure 3.** Velocity-amplitude diagram (Sc = 6).

4. RESPONSE AMPLITUDE

Aerodynamic response amplitude for *Sc* = 6 and 42 are shown in Figs. 3 and 4. The amplitude responses of Rectangular for both *Sc* cases are in good agreement with that reported by Mannini et al. (2016). At *Sc* = 6, motion-induced vortex vibration (MIV), which is also known as one shear layer instability, was observed around the reduced wind velocity of 1.67*B/D* in all sections. In Rectangular and Triple Recession at *Sc* = 6, with relatively large C'_{Fy}, the vibration started from 1/*St*. However, Single Recession, which had been expected to have the lowest onset value due to its high Strouhal number and smallest C'_{Fy}, did not vibrate at 1/*St*.

When *Sc* = 42, the onset in Rectangular with the highest C'_{Fy} was still around 1/*St* and the response amplitude did not show significant changes when compared with *Sc* = 6. In Triple Recession, with moderate C'_{Fy}, the response amplitude notably decreased while the onset was still around 1/*St* like the case of *Sc* = 6. However, in Single Recession, with the smallest C'_{Fy}, the KVIV was not observed and the onset moved into an even higher wind velocity region, which was different from *Sc* = 6 case. Thus, the onsets of Rectangular and Triple Recession were highly controlled by the Kármán vortex, which is also known as two-shear layer instability, as the onsets were around 1/*St* in both *Sc* cases. However, the onset of Single Recession might be influenced by another factor rather than the Kármán vortex as the onset deviated from 1/*St* in both *Sc* cases.

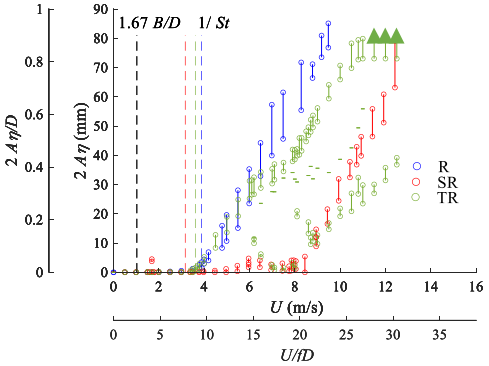

Figure 4. Velocity-amplitude diagram (*Sc* = 42).

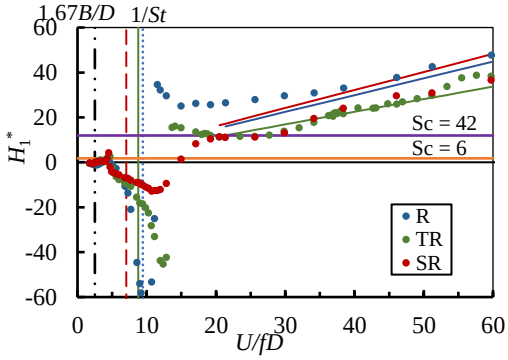

Figure 5. Aerodynamic damping H_1*.

5. AERODYNAMIC DAMPING

Fig. 5 shows Scanlan's flutter derivatives H_1^*, which denotes the vertical aerodynamic damping (Scanlan and Tomko, 1971), of three cylinders. The H_1^* was positive around 1.67*B/D*, which corresponds to MIV. Rectangular, with the highest C'_{Fy}, had the maximum negative H_1^* value at 1/*St*. Then, the sign of H_1^* changed to positive. Thus, Kármán vortex worked as a damping force and controlled the galloping onset. When the C'_{Fy} value was decreased, Triple Recession, the maximum negative H_1^* value decreased while the onset is still around 1/*St*. When C'_{Fy} was smallest, Single Recession, H_1^* was considerably decreased. Moreover, the onset moved into an even higher wind velocity region. This reinforces the remark in section 4, that is the galloping onset of Single Recession might be affected by another phenomenon besides the Kármán vortex.

6. INTERFERENCE BETWEEN VORTICES AND GALLOPING INSTABILITY

Non-dimensional lift amplitudes and phases are shown in Fig. 6. Rectangular with the highest C'_{Fy} had the largest lift amplitude at 1/*St*. For Triple Recession with moderate C'_{Fy}, the lift amplitude peak starting from 1.67*B/D* was larger than that starting from 1/*St*. Thus, motion-induced vortices

became to influence the vibration as the effect of Kármán vortex decreased. However, Kármán vortex still affected the galloping onset in Triple Recession since a clear peak starting from 1/*St* was still observed in the phase lag. Therefore, the galloping onsets of Rectangular and Triple Recession start from 1/*St* in the velocity-amplitude diagrams. In Single Recession, with the lowest C'_{Fy}, motion-induced vortices controlled the galloping onset and vibration because the highest lift amplitude was observed only around 1.67*B/D*. Thus, Single Recession has a higher galloping onset although its 1/*St* is small. To summarize, the Kármán vortex controlled the galloping onset when the Kármán vortex shedding intensity was large. When the Kármán vortex shedding intensity was reduced, the motion-induced vortices dominated the vibration and the galloping onset was moved into higher wind velocity region. A similar phenomenon was also observed when the Kármán vortex was suppressed by attaching a splitter plate to a rectangular cylinder of *B/D* = 2 (Yagi et al., 2013).

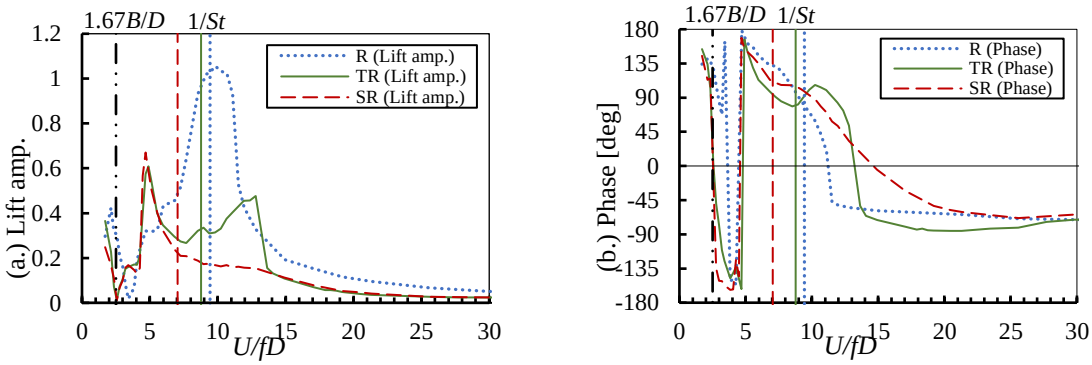

Figure 6. Lift amplitude and phase of R, SR and TR sections.

7. CONCLUSIONS

When the corners of a rectangular cylinder were cut into single and triple recession shapes, the Kármán vortex shedding intensity (C'_{Fy}) was reduced to about 55 % and 86 %. When the Scruton number was small (*Sc* = 6), the galloping onset of Single Recession increased into high wind velocity despite the decrease in 1/*St*. When *Sc* was increased to 42, the galloping onset of Single Recession, with the smallest C'_{Fy}, was further increased into the higher wind velocity region while the galloping onset of other sections remained the same. This is probably because the influence of motion-induced vortices became larger and increased the galloping onset reduced wind velocity as C'_{Fy} was reduced.

ACKNOWLEDGEMENTS

This work was partially supported by JSPS KAKENHI Grant Number 20H02232.

REFERENCES

Scanlan, R. H. and Tomko, J. J., 1971. Airfoil and bridge deck flutter derivatives. Journal of the Engineering Mechanics Division 97, 1717–1737.

Scruton, C., 1968. On the wind-excited oscillation of stacks, towers and mats. International conference on buildings and structures, 1963. Teddington, London, 798–883.

Shiraishi, N., Matsumoto, M., Shirato, H., and Ishizaki, H., 1988. On aerodynamic stability effects for bluff rectangular cylinders by their corner-cut. Journal of Wind Engineering and Industrial Aerodynamics 28, 371–380.

Mannini, C., Marra, A. M., Massai, T., and Bartoli, G., 2016. Interference of vortex-induced vibration and transverse galloping for a rectangular cylinder. Journal of Fluids and Structures 66, 403–423.

Yagi, T., Shinjo, K., Narita, S., Nakase, T., and Shirato, H., 2013. Interferences of vortex sheddings in galloping instability of rectangular cylinders. Journal of Structural Engineering 59A, 552–561 (in Japanese).